Sensitivity Estimates and Backgrounds Studies for Phase-I and II of the COMET Experiment

Benjamin Edward Krikler
of Imperial College London

A dissertation submitted to Imperial College London
for the degree of Doctor of Philosophy

Abstract

Declaration

This dissertation is the result of my own work, except where explicit reference is made to the work of others, and has not been submitted for another qualification to this or any other university. This dissertation does not exceed the word limit for the respective Degree Committee.

Benjamin Edward Krikler

Acknowledgements

Contents

Chapter 1

Phase-II Optimisation

1. Before a substantial sensitivity estimate can be made, need a solidly optimised design

2. Aiming for 3×10^{-17} within a single year of running

3. Designs previously optimised [**?**], and these results are used as nominal design / starting point

4. Fresh optimisation using new software / simulation, updated fieldmaps, physics lists and geometry

5. Some aspects fixed already since Phase-I under construction: Experiment hall, Torus1, detector solenoid, fieldmap and coil parameters?

6. Key areas for optimising:

6.1. Production target dimensions

6.2. Torus1 dipole field strength

6.3. Torus2 dipole field strength

6.4. Electron spectrometer dipole field strength

6.5. collimator shapes and locations

6.6. stopping target and beam blocker position and form

6.7. DIO blockers on spectrometer

1.1 Optimisation Strategy

7. Take some aspects as fixed

8. Limit scope and approach:

8.1. Ideally, each aspect optimised in combination to maximise signal acceptance and reduce background

8.2. How decoupled are each section?

8.3. In practise such an optimisation is not easy to do, instead aim to produce a baseline optimisation so that all backgrounds / issues can be identified

8.4. This can then form basis for further optimisation, with perhaps a smarter more integrated approach

9. Method:

9.1. Production target optimisation

9.1.1. Maximise muon and pion yield between 0 and 80 MeV at entrance to muon beamline

9.1.2. Parameters to vary: target length, target radius

9.2. Muon beam optimisation

9.2.1. Maximise muon stopping rate in stopping target

9.2.2. Minimise pion stopping rate

9.2.3. vary dipole along TS2 and TS4

9.2.4. vary Collimators: TS2 and at TS3

9.3. Electron spectrometer optimisation

9.3.1. Optimise dipole to increase signal acceptance

9.3.2. Optimse DIO blockers so DIO rate per straw is less than 1 kHz

9.3.3. Vary solenoidal field to increase separation?

9.4. Stopping target / beam blocker optimisation

9.4.1. Maximise reflection of signal electrons from upstream by tuning target position

9.5. Detector optimisation

1.2 Optimisation Goals

10. Set sensitivity goal and optimise to reach this

11. Single event sensitivity only considers signal acceptance, but also need to understand backgrounds in terms of final confidence limit that can be set

1.3 Production Target Optimisation

In the Phase-II Conceptual Design Report (CDR), the production target is given as being 16 cm in length and 4 mm in radius [**?**]. Since then, there have been changes to the magnetic field in this region, as well as the lengths and locations of solenoids, shielding and beam-pipe, and the proton beam. Previous studies have looked at comparing the Tungsten target proposed for Phase-II to other materials [**?**], and also drawn a comparison between MARS [**?**], Geant4 [**?**] and the limited data available.

The goal in this study then is to optimise the production target with the up-to-date configurations. This study aims to maximise the total muon and pion yield below 80 MeV at the entrance to the Torus1 bent solenoid, by varying the radius and length of the production target.

1.3.1 Configuration

Table 1.1 gives the key parameters for the beam input and other aspects of this simulation. The location and orientation of the target were held fixed, since the proton beamline is fixed with respect to the muon beam axis. Once a realistic proton beam becomes available, these values would also benefit from optimisation, however. During the scan over length, the back face of the target was kept 8 cm away from the muon beam since the radiation shielding has previously been optimised, and since beyond this the magnetic field will no longer be able to capture the pions and muons produced.

It must be noted that at this point in time there is a appreciable uncertainty in the proton beam profile and position. In particular, whilst the proton beamline upstream has

Proton Beam	
Horizontal spread, σ_x	5.8 mm
Vertical spread, σ_y	2.9 mm
Mean energy, μ_E	8.01 GeV
Energy spread, σ_E	0.135 MeV
Target	
Material	Tungsten
Orientation	10° between target's principal axis and the muon beam axis.
Location	Back face fixed 8 cm away from muon beam axis.
Length	16 cm in CDR. Varied in steps of 4 cm from 4 to 32 cm.
Radius	4 mm in CDR. Varied from 2 to 10 cm in steps of 2 cm and from 10 to 30 cm in steps of 4 cm.
Software configuration	
Packages	`heads/1512w51_develop(3a0ee59)__3_UNCOMMITTED__`
Externals	`heads/Patch_Geant4-G4MultiLevelLocator(11fc8f0)`
Fieldmap	160104 ***((CHECK:))***
Sample Sizes	
Length scan	3e5 Protons on Target (POT) (30 runs of 1e4)
Radius scan	4.9e5 POT (49 runs of 1e4)
Final scan	

Table 1.1: Key parameters in the configuration of the Production Target optimisation.

been well delivered, the effect of the magnetic field and necessary dipole and quadrupole magnetics are still being studied by the proton beam-line group. The beam profile is given in the Phase-I Technical Design Report (TDR) as having a Gaussian profile and energy distribution, but no divergence or location is given. The effect of the proton beam distribution on the overall sensitivity shall therefore be considered later on.

Protons originated from a plane (distributed as a two dimensional Gaussian across this surface) but since there is therefore some scope to tune the proton beam's position, the input particle plane was moved to remain 1 cm away from the front surface of the target. Since the aim is to maximise the muon and pion yield by varying only the length and radius, shifting the proton beam input plane in this way removes any variation of target acceptance due to divergences of the proton beam in the magnetic field.

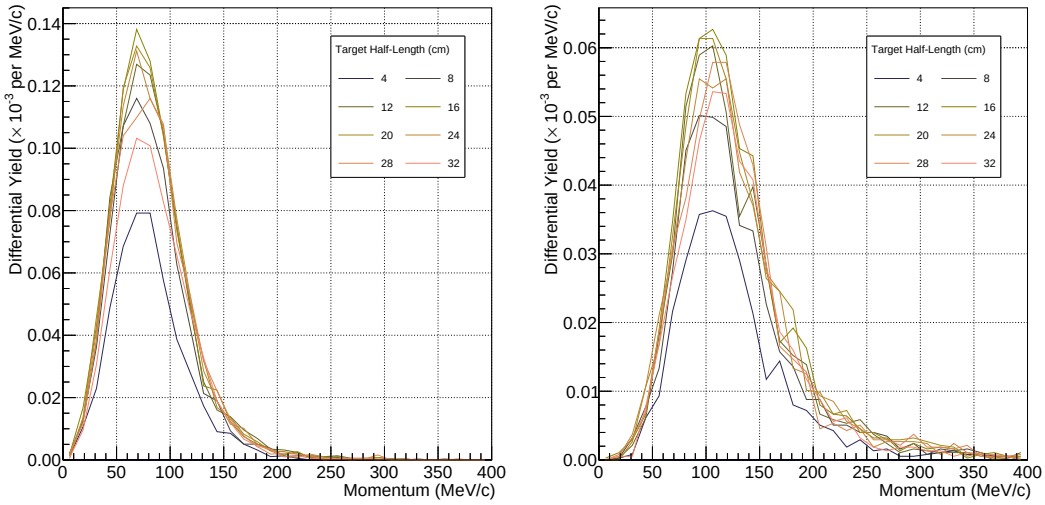

(a) Muons **(b)** Pions

Figure 1.1: Change to momentum distributions at the entrance to the first 90 degrees of the bent muon beam solenoid for different target lengths.

1.3.2 Length Scan

Fig. **??** shows the momentum distributions of pions and muons for different target lengths. Fig. 1.2 then shows these distributions integrated up to different momentum. From these plots it can be seen that the optimum target length occurs around a total length of 32 cm.

Additionally it can be seen

12. Figure of length scan momentum plots

13. Figure of length scan integrals up to a momentum

14. Figure of variation of shape vs length

15. Conclusion

1.3.3 Radius scan

16. Figure of radius scan momentum plots

17. Figure of radius scan integrals up to a momentum

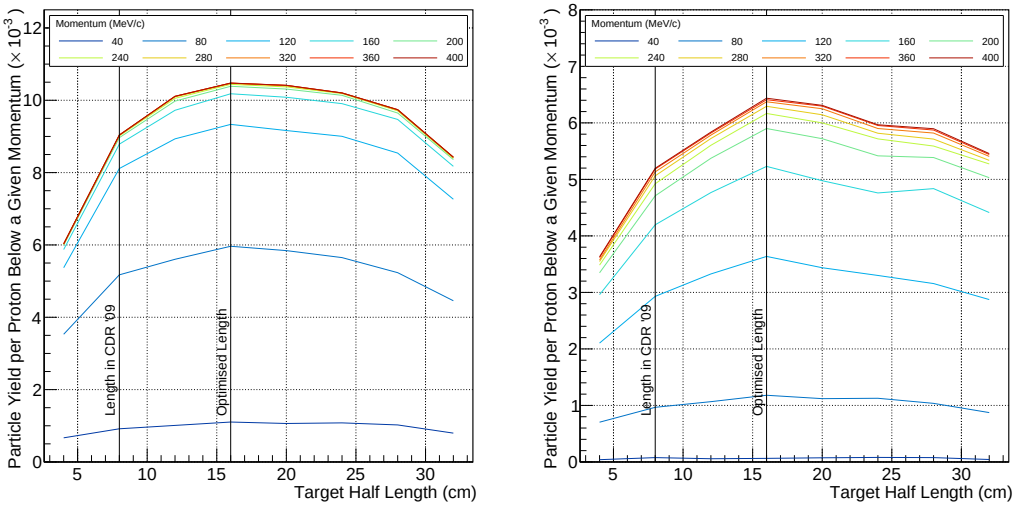

(a) Muons **(b)** Pions

Figure 1.2: Integrated muon and pion yields up to a certain momentum at the entrance to the first 90 degrees of the bent muon beam solenoid as a function of target length.

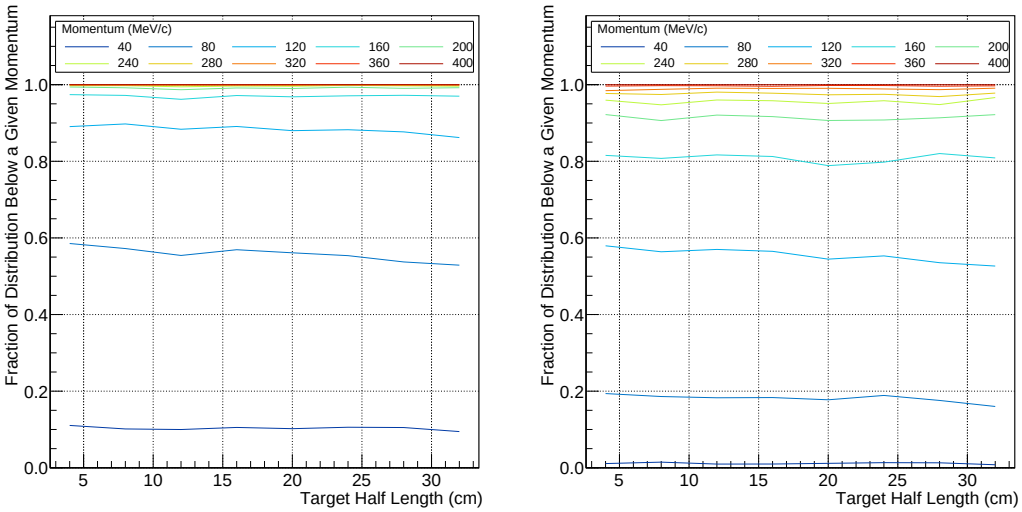

(a) Muons **(b)** Pions

Figure 1.3: Change in the momentum distribution of muons and pions at the entrance to the first 90 degrees of the bent muon beam solenoid as a function of target length.

18. Figure of variation of shape vs radius

19. Conclusion

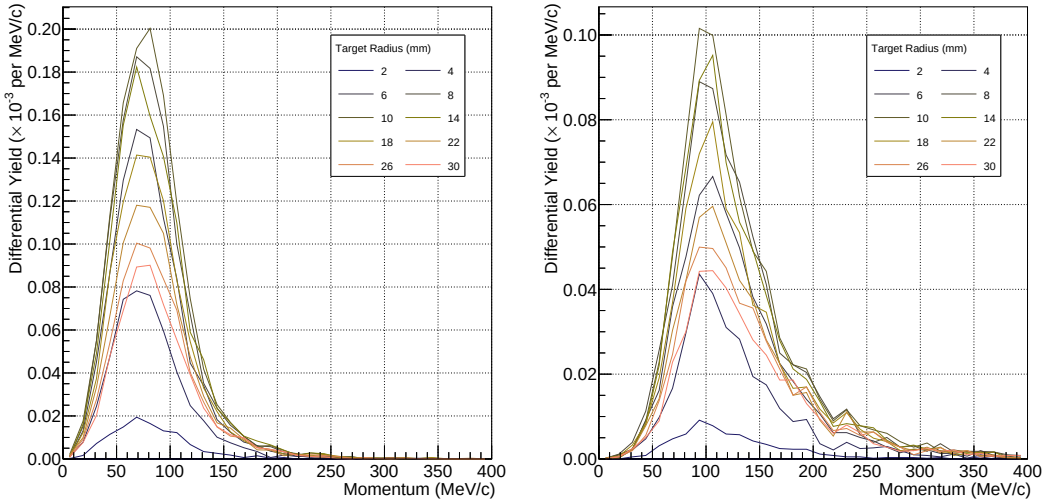

(a) Muons **(b)** Pions

Figure 1.4: Change to momentum distributions at the entrance to the first 90 degrees of the bent muon beam solenoid for different target radii.

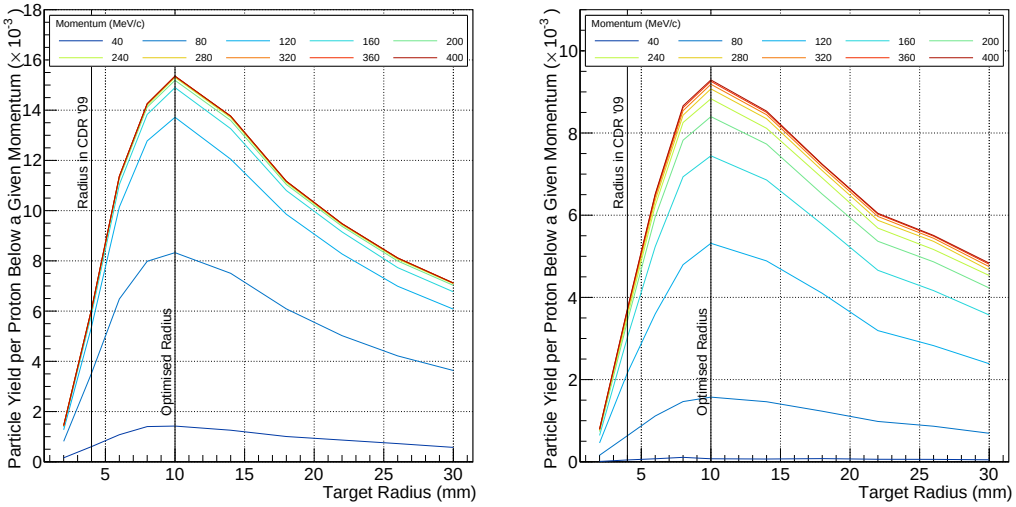

(a) Muons **(b)** Pions

Figure 1.5: Integrated muon and pion yields up to a certain momentum at the entrance to the first 90 degrees of the bent muon beam solenoid as a function of target radius.

1.3.4 Optimised Phase-II

20. Figure comparing Phase-II to Phase-I

21. Conclusions

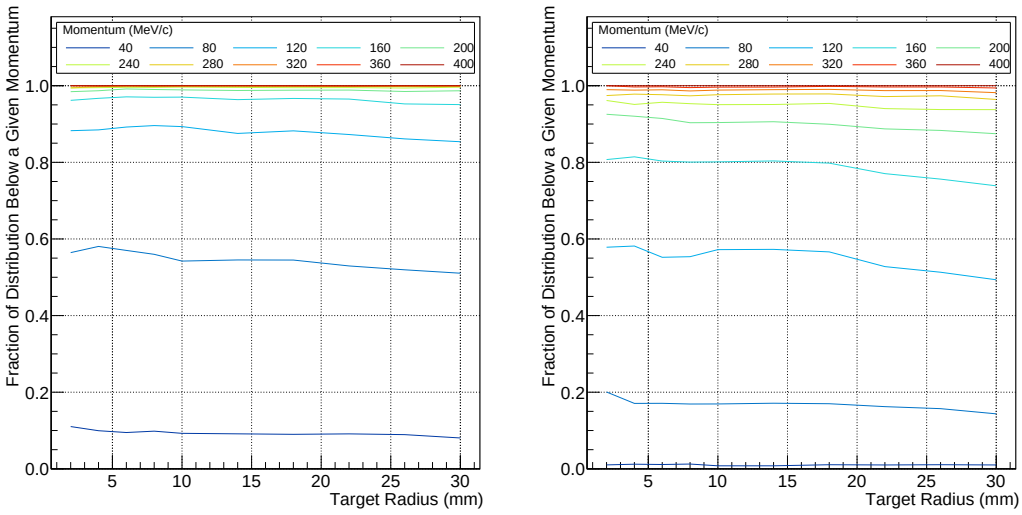

(a) Muons **(b)** Pions

Figure 1.6: Change in the momentum distribution of muons and pions at the entrance to the first 90 degrees of the bent muon beam solenoid as a function of target radius.

List of Acronyms

CDR Conceptual Design Report

POT Protons on Target

TDR Technical Design Report